Hindawi
Mathematical Problems in Engineering
Volume 2022, Article ID 3844771, 10 pages
https://doi.org/10.1155/2022/3844771

Research Article

Study on the Equivalent Permeability Coefficient of Karst Conduit with Single Conduit and Multigroup Fissures

Tianyu Li,[1] Qiuyan Fan ,[2] Pengshuai Yang,[1] and Jiahui Liang[1]

[1]*Research Center of Geotechnical and Structural Engineering, Shandong University, Ji'nan, Shandong 250061, China*
[2]*School of Resources, Environment and Materials, Guangxi University, Nanning, Guangxi 530004, China*

Correspondence should be addressed to Qiuyan Fan; 202186000192@email.sdu.edu.cn

Received 28 February 2022; Accepted 25 March 2022; Published 23 June 2022

Academic Editor: Song Jiang

In order to improve the calculation method of the conversion coefficient of karst conduit under the condition of multiple fissures and conduit intersecting, the indoor test model of karst groundwater seepage with a single conduit and multiple groups of fissures is established. Under the condition of fixed upstream and downstream water heads, the changes of karst conduit water head under different fissures width, fissures combination, and different flow velocity were observed. The test found that the karst conduit water level gradually decreased with the increase of distance, showing an obvious linear relationship. Based on the above-observed water head law, the conversion coefficient of fissures influence is introduced into the Darcy–Weisbach formula, and the regression analysis of test data are used to obtain the calculation formula of the equivalent permeability coefficient of conduit intersecting multiple fissures and karst conduit. The formula is applicable to the case that the fissures are equidistant and the conduit is vertical and does not change dramatically along the conduit.

1. Introduction

Fissures development of underground conduit is very complex in karst areas, and the hydrodynamic characteristics of the groundwater flowing in the fissures are more complex. In view of this feature, some scholars have proposed a triple void medium model regarding karst conduit-fissure-pore [1, 2]. This method puts forward the concept of converted permeability coefficient of fissures and karst conduit, which rationality and superiority have been verified in several practical applications. Although the model considers the mutual exchange between fissure water and conduit water when calculating the converted permeability coefficient of the conduit by Darcy–Weisbach's formula for round pipe flow, the influence of intersecting fissure-conduit water on conduit permeability coefficient is not taken into account [3–5]. In view of this, many scholars have studied the characteristics of flows which come from the intersection of fissure-fissure or fissure-conduit. When groundwater flows in the conduit with fissures, in addition to the local head loss at the intersecting point, the existence of fissure will also affect the flow of the stream in the conduit, resulting in a head loss along the conduit itself [6–8]. It is necessary to take the above-given two factors into account when calculating the converted permeability coefficient of the karst conduit, especially when there are many fissures intersecting along the conduit [9, 10]. Therefore, two groups of indoor test models for the coexistence of vertical fissures and karst conduits are designed in this paper so as to study the value-taking method of conduit conversion permeability coefficient when multiple fissures and karst conduits cross each other.

2. Materials and Methods

2.1. Design of Test Model. In karst developed areas, fissures of underground karst conduits are interlaced and complex, so it is difficult for the test model to fully consider the various geological combinations of fissure-karst conduits [11]. Therefore, this indoor model test only considers the combined karst geological model of two groups of

mutually perpendicular fissures and one karst conduit. The indoor test model can be divided into four parts: water supply system, in which water from nearby lakes is pumped by submersible pumps and enters the water supply tank; monitoring system, which is a row of observation hole preset above the conduit, and the observation hole is connected with the conduit and the fissures nearby, and the water level of the conduit in the flow field can be directly measured by a steel tape; water storage system, in which the water discharged through the conduit enters the overflow tank and then flows into the water tank, and the water discharge will be recorded by reading the water level and bottom area of the water tank; rock mass model, including rock block, karst conduit and two groups of fissures which are perpendicular to each other, simulates rock block by the module bonded with acrylic board (i.e., without considering seepage inside rock block), simulates karst fissure by space between modules (two surfaces of crack are parallel to each other and the distance remains constant), and simulates karst conduit by presetting round pipes in the module (the pipe is straight and its diameter remains unchanged) [12–15]. The pipe is separated by vertical fissures, and water in the fissure and water in the pipe can be exchanged with each other in the process of groundwater flowing [16]. The design and physical drawings of this device are shown in Figures 1 and 2.

2.2. Material Dimensions and Design of Working Conditions. The diameter of the pipe is 10 cm, and the center of the pipe is 7.5 cm away from the bottom surface, crossing the vertical fissure vertically. In order to obtain a stable water level in the pipe fissures, the water levels at the inlet/outlet are set changeless in this test. The design upstream water level is 50 cm and the design downstream water level is 25 cm. Therefore, the baffle plate for upstream and downstream is 50 cm and 25 cm, respectively, so as to control the upstream and downstream water levels. The plane dimension of the water supply tank is 1.0 m in length and 1.0 m in width; the overflow conduit is 0.5 m in length and 1.0 m in width.

The mutually perpendicular fissure groups are designed with two different spaces of 25×15 cm and 50×30 cm, respectively, which are denoted with dense/thin respectively for the convenience to express. The horizontal and vertical width of the fissure is 1 mm, 3 mm, and 5 mm, respectively, and combinations of horizontal and vertical fissures are made. For the convenience of expression, it will be denoted directly in form of horizontal $(H)^*$ and vertical $(V)^*$. Its front and side schematic diagrams are as shown in Figures 3–6. The tail end of the pipe is provided with a card slot, which can achieve the purpose of controlling the flow rate of water in the pipe by way of placing different baffles to control the inlet/outlet size of the pipe. The card slot and baffle are shown in Figures 7 and 8. The test conditions eventually obtained are shown in Table 1. The baffle setting of 0 in the table refers to conditions without baffle placing.

2.3. Layout and Spacing of Observation Hole. The observation hole is directly connected with the pipe. One observation hole is connected with vertical and horizontal fissures, respectively, (e g., observation hole 1), whereas the other observation hole only intersects with the horizontal fissure (e g., observation hole 2). The layout of the observation hole is shown in Figure 9. The longitudinal spacing (along the water flow direction) of the observation hole varies with different working conditions. The longitudinal spacing of the observation hole under different working conditions is listed in Table 2 (taking the H5V5dense as an example). The starting point of each distance measurement in the table is the front end of the module in the water supply tank, and its unit is cm.

3. Result and Analysis

When the water level in the upstream and downstream as well as in the observation hole is stable, the water levels of the observation hole under different working conditions are drawn into a curve graph, as shown in Figures 10–19. The vertical coordinate represents the water level, and the unit is expressed in centimeters. The horizontal coordinate represents the distance between each observation hole and the upstream water supply tank, and its unit is expressed in centimeters.

The number of observation holes along the axis of X direction is 1, 2, 3, 4, and 5 in turn, among which observation hole No.1 was closest to the upstream water supply tank with the highest water level, and observation hole No.5 was closest to the downstream overflow tank with the lowest water level. At the same time, when the upstream and downstream water levels as well as the water level in the observation hole are stable, the height Δh_b and time t of water level increase in the water tank can be recorded. The bottom area s_b of the tank was measured as 3.0177m^{2}and the pipe diameter d as 10 cm. Since the upstream and downstream water levels are changeless, when the water level of the observation hole is stable, the average flow velocity in the pipe makes little change. The average flow velocity in the pipe can be calculated by the following formula:

$$v = \frac{\left(\Delta h_b \cdot s_b / t\right)}{\left(\pi \cdot d^2/4\right)}. \tag{1}$$

The results are shown in Table 3.

As shown in Figures 10–19, under various working conditions and flow velocity, the groundwater level in the conduit decreases gradually with the increase of distance, showing a significant linear relationship. Besides, the faster the water flows in the conduit, the greater the head loss along the pipe. The above-given law is in consistent with Darcy–Weisbach formula of head loss for common pipe flow [17].

$$h_f = \lambda \cdot \left(\frac{L}{d_i}\right) \cdot \left(\frac{v^2}{2g}\right). \tag{2}$$

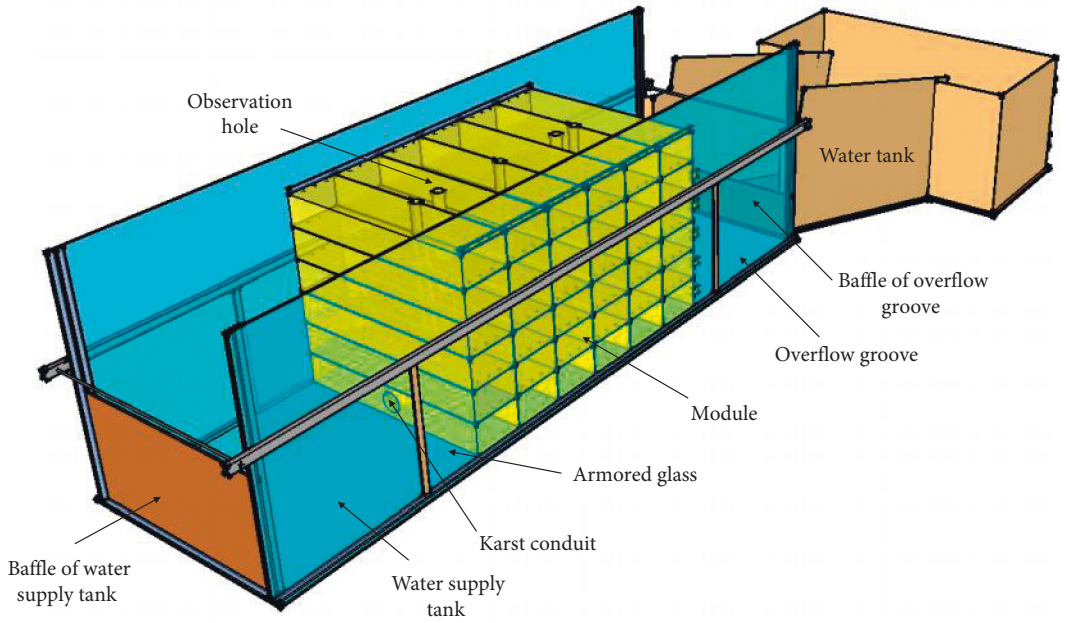

Figure 1: Design drawing of the indoor test model.

Figure 2: Physical diagram of the test model.

Here, λ represents the hydraulic friction coefficient, L represents the length(m) of the pipe, d_i represents the inner diameter(m) of the pipe, V represents the average flow velocity (m/s), and g represents gravity acceleration, which is 9.81 m/s^2.

As defined by *the Outdoor Water Supply Design Specification* [18], for the round pipes with a smooth plastic wall, its hydraulic friction coefficient λ should be calculated according to the following formula:

$$\lambda = \frac{0.304}{R_e^{0.239}}. \tag{3}$$

Here, R_e represents the Reynolds number.

In this paper, the acrylic board is used to simulate the underground karst conduit and the inner wall of the fissure system which is relatively smooth, but due to the existence of transverse and vertical fissures, it may be unsuitable to calculate the head loss along the conduit by the above-given formula. Therefore, it is also necessary to additionally consider the coefficient resulting from fissure influence in the hydraulic friction coefficient λ.

Making h_h represents the fissure's width, h_v for its vertical width, s_h for its horizontal width, s_v for the its vertical spacing, and γ for kinematic coefficient of viscosity (taken as 1.31×10^{-6} m^3/s when the test water temperature is about 10 °C). Therefore, $v \cdot h_h/\gamma$ is defined as the influence

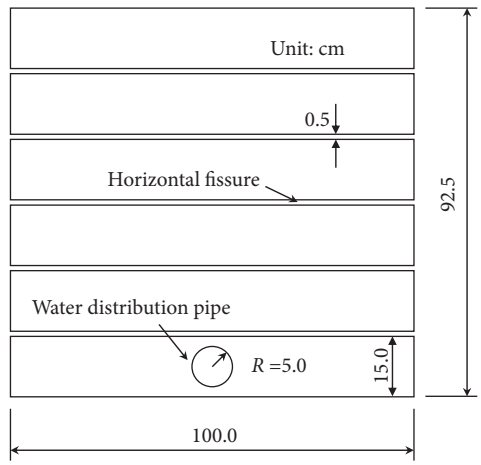

Figure 3: Front view of horizontal and vertical fissure module with a spacing of 25 × 15 cm.

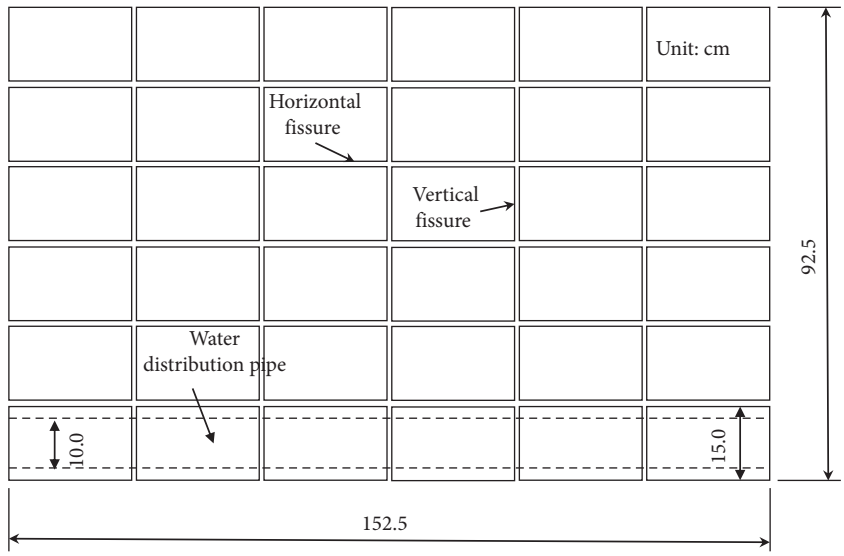

Figure 4: Side view of horizontal and vertical fissure module with a spacing of 25 × 15 cm.

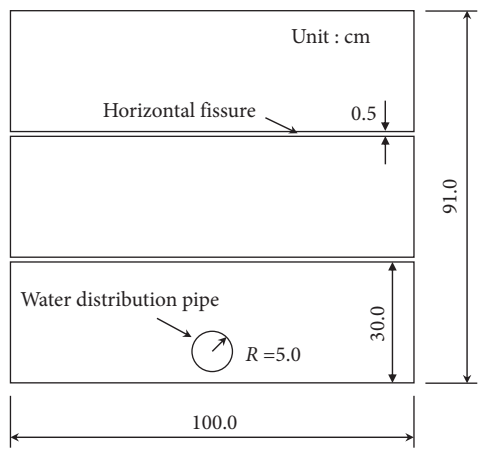

Figure 5: Front view of horizontal and vertical fissure module with a spacing of 50 × 30 cm.

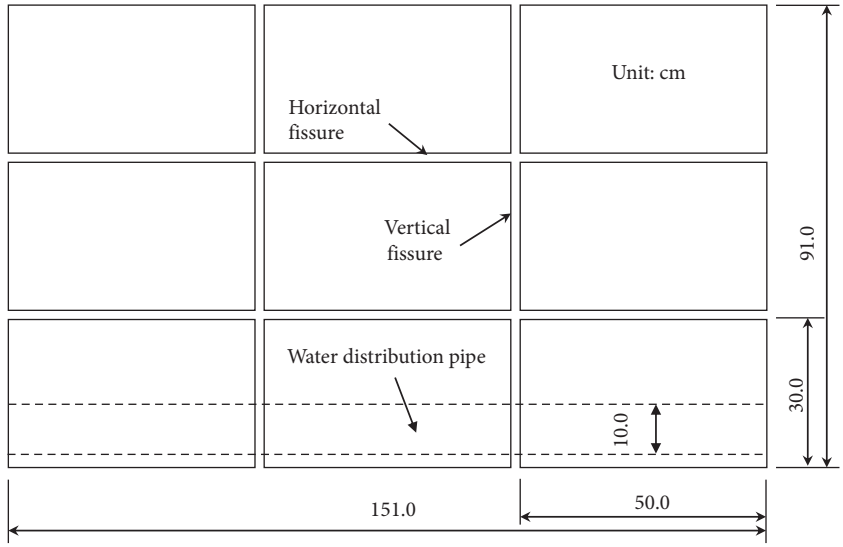

Figure 6: Side view of horizontal and vertical fissure module with a spacing of 50 × 30 cm.

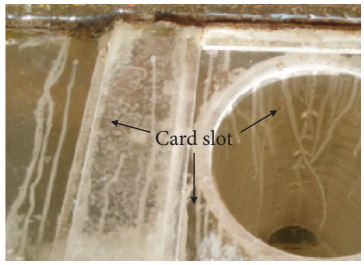

Figure 7: Card slot.

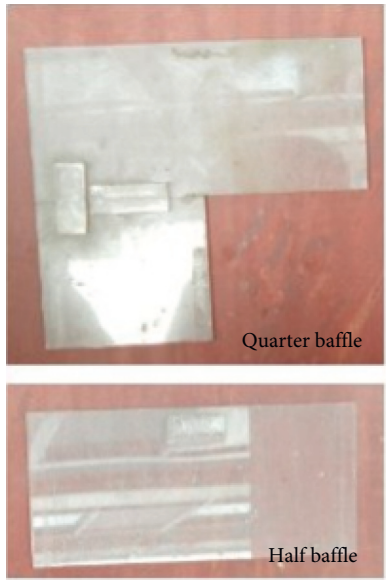

Figure 8: Baffle plate.

coefficient of horizontal fissure width, $v \cdot h_h/\gamma$ as the influence coefficient of vertical fissure width, $v \cdot s_v/\gamma$ as the influence coefficient of vertical fissure space, and $v \cdot s_h/\gamma$ as the influence coefficient of horizontal fissure space. All the above-given variables are dimensionless coefficients, thus the overall fissure influence coefficient is

$$\lambda_f = e \cdot \left(\frac{v \cdot h_v}{\gamma}\right)^a \cdot \left(\frac{v \cdot h_h}{\gamma}\right)^b \cdot \left(\frac{v \cdot s_v}{\gamma}\right)^c \cdot \left(\frac{v \cdot s_h}{\gamma}\right)^d. \quad (4)$$

Here, a, b, c, d, and e are all constant coefficient to be solved.

Then, the calculation formula of head loss of the pipe with horizontal and vertical fissures is

$$h_f' = \lambda_f \cdot \lambda \cdot \frac{L}{d_i} \cdot \frac{v^2}{2g}. \quad (5)$$

The formula to calculate the converted permeability coefficient of the pipe with horizontal and vertical fissures is

$$K_L = \lambda_f \cdot \lambda \cdot \frac{v^2}{2d_i g}. \quad (6)$$

In order to verify the rationality of the added coefficient, and meanwhile, to obtain the value of each constant coefficient in fissures correction coefficient, fitting calculation can be made by the unit loss of head measured by the above-given test (the slope of the head curve in Figures 10–19) together with formula (6). See following Table 3 for the value of each parameter.

After iterative calculation, if there is a coefficient with a of −0.232, b of −0.109, c of −0.061, d of −0.055, and e of 106, it will demonstrate a good fitting effect with the

Table 1: Test conditions.

Test conditions										
Space	25 × 15 cm (dense)					50 × 30 cm (thin)				
Baff	¼		½		0	¼		½		0
Combinations	H1V1	H1V5	H3V3	H5V1	H5V5	H1V1	H1V5	H3V3	H5V1	H5V5

Table 2: Observation hole distance.

Working conditions	Observation hole number on longitudinal main pipe				
	1	2	3	4	5
H1V1dense	25	37.5	75.1	112.7	125.2
H1V5thin	25	37.5	75.1	112.7	125.2
H3V3thin	25	37.5	75.3	113.1	125.6
H5V1 thin	25	37.5	75.5	113.5	126.0
H5V5thin	25	37.5	75.5	113.5	126.0
H1V1dense	25.05	37.6	75.25	112.9	125.45
H1V5dense	25.05	37.6	75.25	112.9	125.45
H3V3dense	25.15	37.8	75.75	113.7	126.35
H5V1dense	25.25	38.0	76.25	114.5	127.25
H5V5dense	25.25	38.0	76.25	114.5	127.25

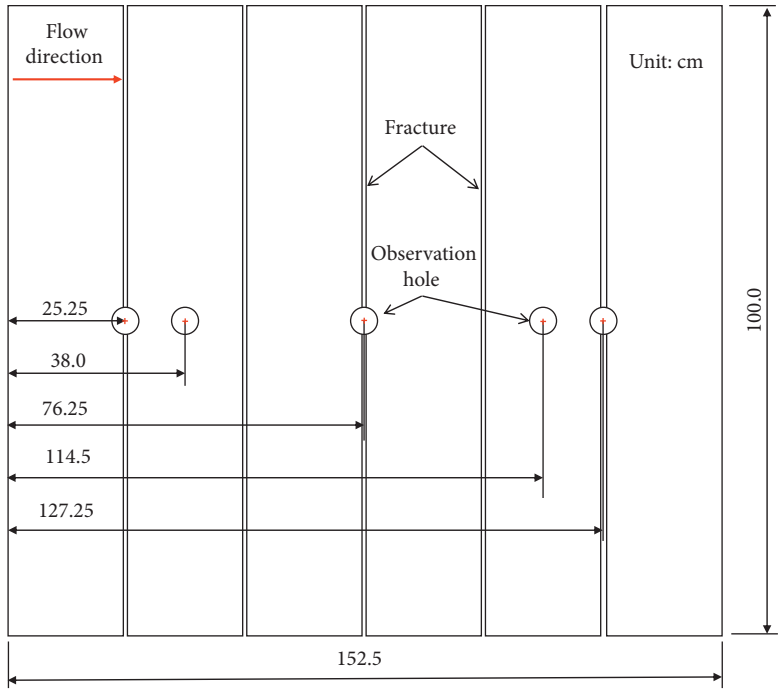

Figure 9: Horizontal 5 Vertical 5 dense, schematic diagram of the distance between observation holes.

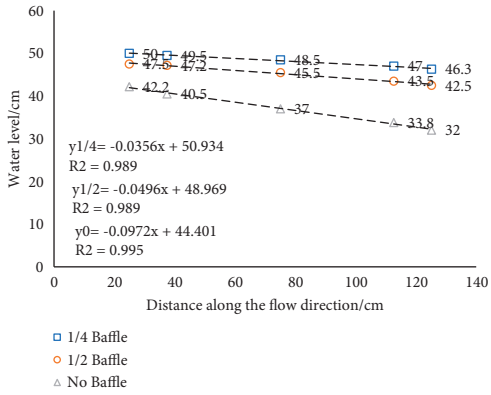

Figure 10: Horizontal 1 vertical 1 combined observation hole water level curve.

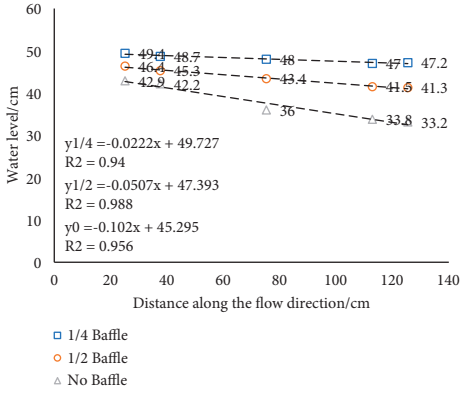

Figure 11: Horizontal 1 vertical 1 divided observation hole water level curve.

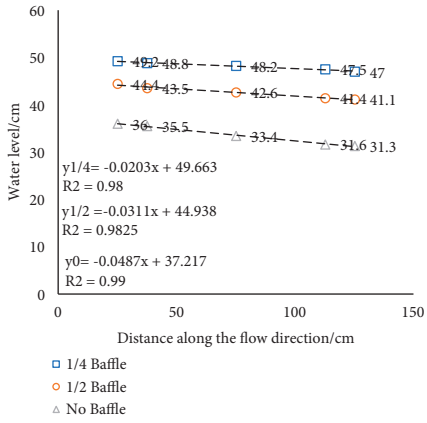

Figure 12: Horizontal 1 vertical 5 combined observation hole water level curve.

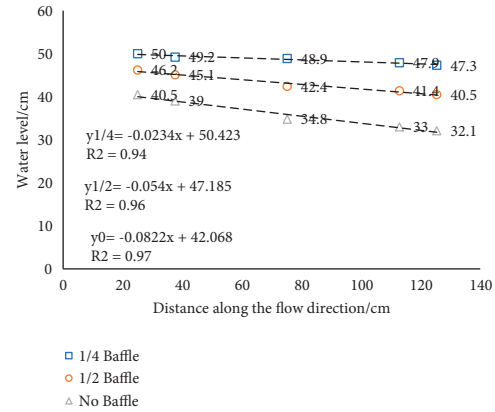

Figure 13: Horizontal 1 vertical 5 divided observation hole water level curve.

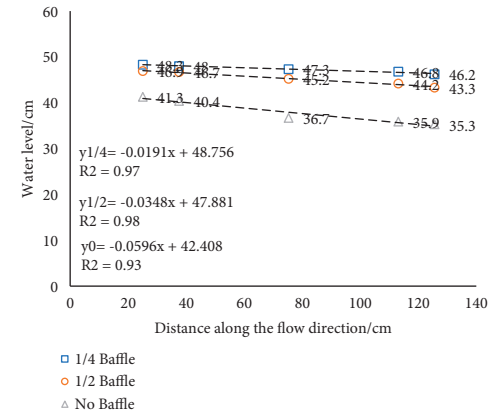

Figure 14: Horizontal 3 vertical 3 combined observation hole water level curve.

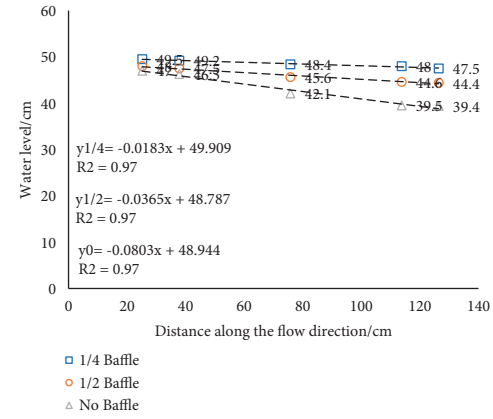

Figure 15: Horizontal 3 vertical 3 divided observation hole water level curve.

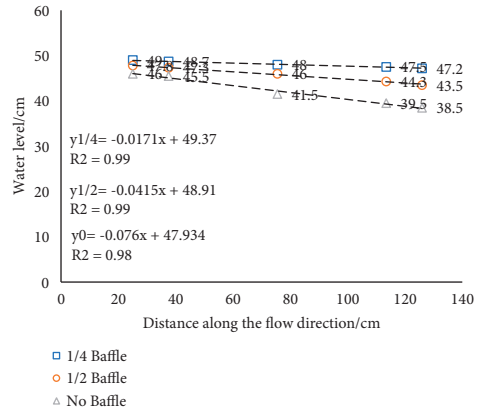

Figure 16: Horizontal 5 vertical 1 combined observation hole water level curve.

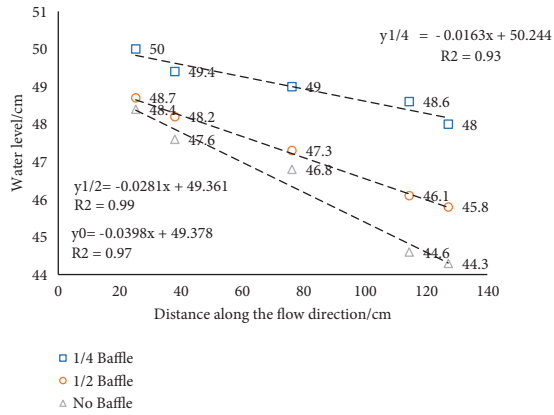

Figure 17: Horizontal 5 vertical 1 divided observation hole water level curve.

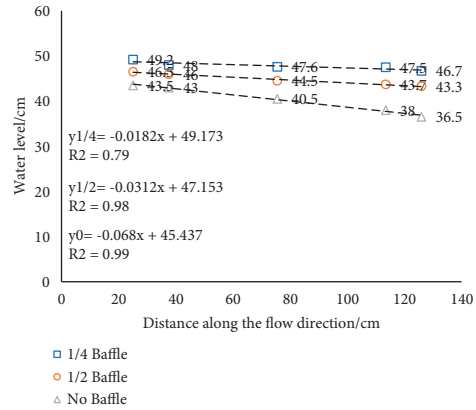

Figure 18: Horizontal 5 vertical 5 combined observation hole water level curve.

related parameters $R^2 = 0.84$, and the sum of the squares of the residuals of 0.00282. The calculated unit head loss is shown in Table 3. The revised calculation formula of converted permeability coefficient of karst conduit is applicable to the case that the fissures are distributed at equal intervals and the conduit keeps vertical and does not suffers from dramatically changes along the route. In the actual observation process, and in the local areas, the groundwater flow velocity or the equivalent radius of the flow area can be calculated by the above formula and

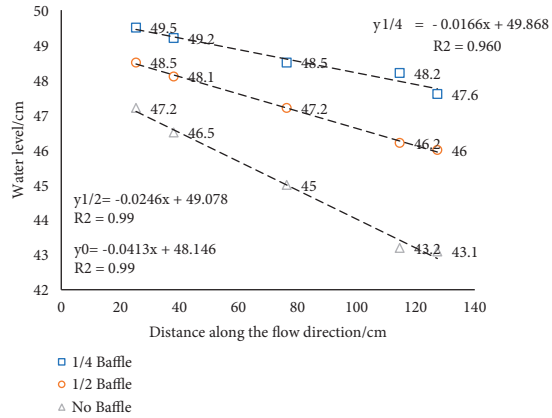

Figure 19: Horizontal 5 vertical 5 divided observation hole water level curve.

Table 3: Fitting parameters and laboratory measurement data.

Working conditions	Flow rate (m/s)	h_h (m)	h_v (m)	s_h (m)	s_v (m)	Measured unit head loss	Calculated unit head loss
H1V1thin1/4 BP	0.879065	0.001	0.001	0.3	0.5	0.0356	0.0229
H1V1 thin 1/2 BP	1.792921	0.001	0.001	0.3	0.5	0.0496	0.0579
H1V1 thin 0 BP	2.577089	0.001	0.001	0.3	0.5	0.0972	0.0929
H1V5 thin 1/4 BP	0.713626	0.001	0.005	0.3	0.5	0.0203	0.0146
H1V5 thin 1/2 BP	1.58838	0.001	0.005	0.3	0.5	0.0311	0.0415
H1V5 thin 0 BP	2.35036	0.001	0.005	0.3	0.5	0.0487	0.0691
H3V3 thin 1/4 BP	0.77065	0.003	0.003	0.3	0.5	0.0191	0.0132
H3V3 thin 1/2 BP	1.681575	0.003	0.003	0.3	0.5	0.0348	0.0366
H3V3 thin 0 BP	2.468152	0.003	0.003	0.3	0.5	0.0596	0.0603
H5V1 thin 1/4 BP	0.760998	0.005	0.001	0.3	0.5	0.0171	0.0130
H5V1 thin 1/2 BP	1.714453	0.005	0.001	0.3	0.5	0.0415	0.0376
H5V1 thin 0 BP	2.536713	0.005	0.001	0.3	0.5	0.076	0.0626
H5V5 thin 1/4 BP	0.745979	0.005	0.005	0.3	0.5	0.0182	0.0107
H5V5 thin 1/2 BP	1.658404	0.005	0.005	0.3	0.5	0.0312	0.0302
H5V5 thin 0 BP	2.503013	0.005	0.005	0.3	0.5	0.068	0.0516
H1V1dense1/4 BP	0.779194	0.001	0.001	0.15	0.25	0.0222	0.0212
H1V1 dense 1/2 BP	1.732893	0.001	0.001	0.15	0.25	0.0507	0.0600
H1V1 dense 0 BP	2.495932	0.001	0.001	0.15	0.25	0.102	0.0966
H1V5 dense 1/4 BP	0.657278	0.001	0.005	0.15	0.25	0.0234	0.0142
H1V5 dense 1/2 BP	1.596411	0.001	0.005	0.15	0.25	0.054	0.0452
H1V5 dense 0 BP	2.357255	0.001	0.005	0.15	0.25	0.0822	0.0752
H3V3 dense 1/4 BP	0.691107	0.003	0.003	0.15	0.25	0.0183	0.0125
H3V3 dense 1/2 BP	1.647228	0.003	0.003	0.15	0.25	0.0365	0.0386
H3V3 dense 0 BP	2.443183	0.003	0.003	0.15	0.25	0.0803	0.0645
H5V1 dense 1/4 BP	0.737937	0.005	0.001	0.15	0.25	0.0163	0.0136
H5V1 dense 1/2 BP	1.598881	0.005	0.001	0.15	0.25	0.0281	0.0372
H5V1 dense 0 BP	2.385524	0.005	0.001	0.15	0.25	0.0398	0.0627
H5V5 dense 1/4 BP	0.688778	0.005	0.005	0.15	0.25	0.0166	0.0104
H5V5 dense 1/2 bp	1.63933	0.005	0.005	0.15	0.25	0.0246	0.0322
H5V5 dense 0 bp	2.368597	0.005	0.005	0.15	0.25	0.0413	0.0521

(Notes: BP-baffle plate).

through measuring a series of changes in the water level of the observation holes.

4. Conclusions

Based on the indoor model test on the flow characteristics of groundwater with a single conduit and multigroup of fissures in karst areas, this paper studies the variation of water level of observation hole on the main drainage pipe under different working conditions and also revised the hydraulic friction coefficient of a round pipe flowing with the test data. The following main conclusions have been obtained:

(1) The groundwater level in the karst conduit decreases gradually with the increase of distance, showing an obvious linear relationship. Moreover, the faster the flow velocity in the conduit, the more the head loss

along the conduit. This law is consistent with Darcy–Weisbach formula of head loss for common pipe flow.

(2) The influence coefficient regarding fissures is added into the hydraulic friction coefficient, and the reduced permeability coefficient of the conduit under conditions of horizontal and vertical fissures has been obtained via fitting the test data. The calculation formula is (7)

$$\begin{cases} K_L = \lambda_f \cdot \lambda \cdot \dfrac{v^2}{2d_i g}, \\ \lambda_f = e \cdot \left(\dfrac{v \cdot h_v}{\gamma}\right)^a \cdot \left(\dfrac{v \cdot h_h}{\gamma}\right)^b \cdot \left(\dfrac{v \cdot s_v}{\gamma}\right)^c \cdot \left(\dfrac{v \cdot s_h}{\gamma}\right)^d. \end{cases} \tag{7}$$

The value of a, b, c, d, and e is obtained by regression analysis.

Data Availability

The figures and tables used to support the findings of this study are included in the article.

Conflicts of Interest

The authors declare that they have no conflicts of interest.

Acknowledgments

The authors thank all the technicians who have contributed to this research.

References

[1] H. Sun, X. Liu, Z. Ye, and E. Wang, "Experimental investigation of the nonlinear evolution from pipe flow to fissure flow during carbonate rock failures," *Bulletin of Engineering Geology and the Environment*, vol. 80, no. 6, pp. 4459–4470, 2021.

[2] J. M. Cheng and C. X. Chen, "An integrated linear/non-linear flow model for the conduit-fissure-pore media in the karst triple void aquifer system," *Environmental Geology*, vol. 47, no. 2, pp. 163–174, 2005.

[3] J. D. Valiantzas, "Explicit power formula for the Darcy-weisbach pipe flow equation: application in optimal pipeline design," *Journal of Irrigation and Drainage Engineering*, vol. 134, no. 4, pp. 454–461, 2008.

[4] T. Haktanır and M. Ardıçlıoğlu, "Numerical modeling of Darcy-Weisbach friction factor and branching pipes problem," *Advances in Engineering Software*, vol. 35, no. 12, pp. 773–779, 2004.

[5] C. H Shin and W. G. Park, "Expansion of the Darcy-Weisbach relation for porous flow analysis," *Transactions of the Korean Society of Mechanical Engineers B*, vol. 41, no. 4, pp. 229–238, 2017.

[6] R. A. Chilton and R. Stainsby, "Pressure loss equations for laminar and turbulent non-Newtonian pipe flow," *Journal of Hydraulic Engineering*, vol. 124, no. 5, pp. 522–529, 1998.

[7] S. Demir, S. Duman, N. Manav Demir, A. Karadeniz, and E. Lubura, "An MS excel add-in for teaching hydraulics of pipe flow in engineering curricula," *Computer Applications in Engineering Education*, vol. 26, no. 3, pp. 449–459, 2018.

[8] A. Bergant, A. Ross Simpson, and J. Vìtkovsk, "Developments in unsteady pipe flow friction modelling," *Journal of Hydraulic Research*, vol. 39, no. 3, pp. 249–257, 2001.

[9] H. J. Kwon, "Analysis of transient flow in a piping system," *KSCE Journal of Civil Engineering*, vol. 11, no. 4, pp. 209–214, 2007.

[10] M. W. Smith, N. J. Cox, and L. J. Bracken, "Applying flow resistance equations to overland flows," *Progress in Physical Geography: Earth and Environment*, vol. 31, no. 4, pp. 363–387, 2007.

[11] S. Ahmed and P. J. Carpenter, "Geophysical response of filled sinkholes, soil pipes and associated bedrock fractures in thinly mantled karst, east-central Illinois," *Environmental Geology*, vol. 44, no. 6, pp. 705–716, 2003.

[12] Z. Mohammadi, W. A. Illman, and M. Field, "Review of laboratory scale models of karst aquifers: approaches, similitude, and requirements," *Ground Water*, vol. 59, no. 2, pp. 163–174, 2021.

[13] F. Xue, M. Cai, T. Wang, and T. Zhao, "Characteristics of karst cave development in urban karst area and its effect on the stability of subway tunnel construction," *Advances in Civil Engineering*, vol. 2021, Article ID 8894713, 12 pages, 2021.

[14] C. Jiang, H. Han, H. Xie, J. Liu, Z. Chen, and H. Chen, "Karst aquifer water inflow into tunnels: an analytical solution," *Geofluids*, vol. 202110 pages, Article ID 6672878, 2021.

[15] F. Wan, P. Xu, P. Zhang, H. Qu, L. Wang, and X. Zhang, "Quantitative inversion of water-inrush incidents in mountain tunnel beneath a karst pit," *Advances in Civil Engineering*, vol. 2021, Article ID 9971944, 18 pages, 2021.

[16] S. Xiao, C. Zeng, J. Lan et al., "Hydrochemical characteristics and controlling factors of typical dolomite karst basin in humid subtropical zone," *Geofluids*, vol. 202114 pages, Article ID 8816097, 2021.

[17] G. O. Brown, "The history of the Darcy-weisbach equation for pipe flow resistance," *American Society of Civil Engineers*, vol. 4, pp. 34–43, 2002.

[18] S. Chen, B. Li, S. Lin et al., "Change of urinary fluoride and bone metabolism indicators in the endemic fluorosis areas of southern China after supplying low fluoride public water," *BMC Public Health*, vol. 13, no. 1, p. 156, 2013.